Research article

Drug Testing and Analysis

Received: 29 July 2014 Revised: 10 September 2014 Accepted: 17 September 2014 Published online in Wiley Online Library

(www.drugtestinganalysis.com) DOI 10.1002/dta.1731

Synthetic cannabimimetic agents metabolized by carboxylesterases

Ragnar Thomsen,[a]* Line M. Nielsen,[a] Niels B. Holm,[a] Henrik B. Rasmussen,[b] Kristian Linnet[a] and the INDICES Consortium[c]

Synthetic cannabimimetic agents are a large group of diverse compounds which act as agonists at cannabinoid receptors. Since 2004, synthetic cannabinoids have been used recreationally, although several of the compounds have been shown to cause severe toxicity in humans. In this study, the metabolism of two indazole carboxamide derivatives, AB-PINACA and AB-FUBINACA, was investigated by using human liver microsomes (HLM). For both compounds, a major metabolic pathway was the enzymatic hydrolysis of the primary amide, resulting in the major metabolites AB-PINACA-COOH and AB-FUBINACA-COOH. Other major metabolic pathways were mono-hydroxylation of the N-pentyl chain in AB-PINACA and mono-hydroxylation of the 1-amino-3-methyl-1-oxobutane moiety in AB-FUBINACA. To identify the enzyme(s) responsible for the amide hydrolysis, incubations with recombinant carboxylesterases and human serum, as well as inhibition studies in HLM and human pulmonary microsomes (HPM) were performed. Carboxylesterase 1 (CES1) was identified as the major human hepatic and pulmonary enzyme responsible for the amide hydrolysis.We employed similar studies to identify the esterase(s) involved in the previously described hydrolytic metabolism of two quinolineindole synthetic cannabinoids, PB-22 and 5F-PB-22, as well as the closely related compound, BB-22. Our investigations again revealed CES1 to be the key enzyme catalyzing these reactions. The identified major metabolites of AB-PINACA and AB-FUBINACA are likely to be useful in documenting drug usage in forensic and clinical screening. Additionally, the identification of CES1 as the main enzyme hydrolyzing these compounds improves our knowledge in the emerging field of xenobiotic metabolism by esterases.

Additional supporting information may be found in the online version of this article at the publisher's web site.

Keywords: synthetic cannabinoids; metabolism; carboxylesterase; human liver microsomes

Introduction

Since the isolation and structure elucidation of the main psychoactive agent in *Cannabis sativa*, (−)-trans-Δ^9-tetrahydrocannabinol (THC) in 1964,[1] research has been ongoing for synthesizing compounds, which lack the undesired psychoactive properties of THC, but retain the therapeutically desired anticonvulsive, analgesic, and antiemetic properties. THC exerts its main effects through binding to cannabinoid receptors, of which two are currently acknowledged, CB_1 and CB_2.[2,3] Several groups of compounds acting as agonists at these receptors, so-called cannabimimetic agents, have since been synthesized. Classic synthetic cannabinoids, such as HU-210 and CP47,497, are structural analogues of THC, while some of the newer compounds, such as JWH-018 and JWH-073 (Figure 1), do not have obvious structural similarities to THC.

Synthetic cannabinoids were first detected in herbal smoking mixtures in 2008,[4–6] but they are likely to have been available for purchase on websites as far back as 2004.[4] Alongside their increased usage, reports of intoxication and dependence began appearing.[7] This led to scheduling of certain synthetic cannabinoids in several countries. Initially, governments banned the most prevalent compounds, which led to a replacement by similar compounds with minor modifications of substituent groups. In an attempt to counteract this trend, some governments have banned entire groups of related compounds by scheduling core substructures, which can have varying attached substituents. As an example, Denmark scheduled seven classes of synthetic cannabinoids in 2012.[8] To circumvent the legislation, manufacturers of synthetic cannabinoids have changed to compounds containing chemical modifications of the core structure. In this ongoing race between legislators and clandestine chemists, some of the newer groups of compounds are the quinolineindoles and indazole carboxamide derivatives.

BB-22, PB-22, and 5F-PB-22 are quinolineindoles, which are characterized by containing a quinoline substructure linked to the 3-position of an indole group by an ester bond (Figure 1). PB-22, also known as QUPIC, was first detected by Finnish Customs in 2012,[9] and the recreational use of PB-22 and BB-22 was reported

* *Correspondence to: Ragnar Thomsen, Section of Forensic Chemistry, Department of Forensic Medicine, Faculty of Health Sciences, University of Copenhagen, Frederik V's vej 11, DK-2100 Copenhagen, Denmark. E-mail: ragnar.thomsen@sund.ku.dk*

a *Section of Forensic Chemistry, Department of Forensic Medicine, Faculty of Health Sciences, University of Copenhagen, Frederik V's vej 11, DK-2100, Copenhagen, Denmark*

b *Institute of Biological Psychiatry, Mental Health Centre Sct. Hans, Copenhagen University Hospital, Boserupvej 2, DK-4000, Roskilde, Denmark*

c *See appendix for a list of all partners in the consortium*

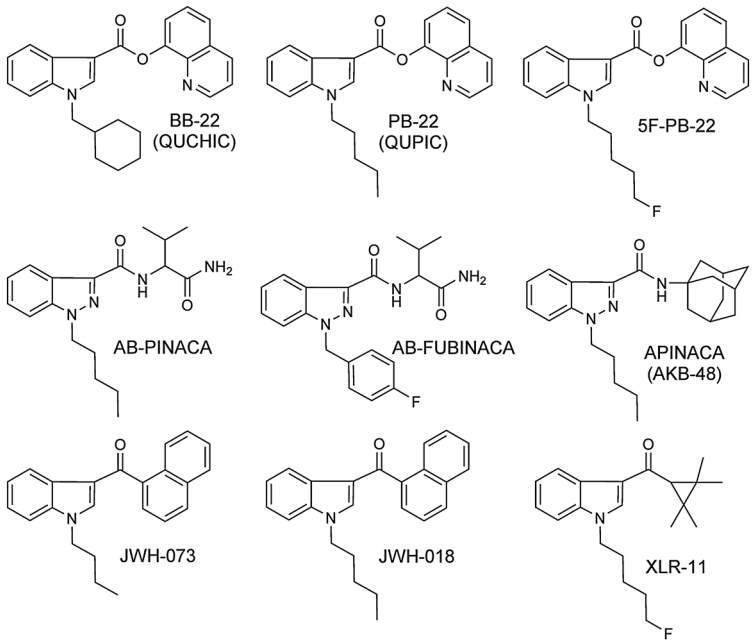

Figure 1. Chemical structures of selected synthetic cannabimimetic agents

in Japan in 2013.[10] In the USA, 5F-PB-22 was found to be involved in four deaths in 2013.[11]

AB-PINACA and AB-FUBINACA, with the full chemical names of *N*-(1-amino-3-methyl-1-oxobutan-2-yl)-1-pentyl-1*H*-indazole-3-carboxamide and *N*-(1-amino-3-methyl-1-oxobutan-2-yl)-1-(4-fluorobenzyl)-1*H*-indazole-3-carboxamide, respectively, are indazole carboxamide derivatives characterized by containing a carboxamide in the 3-position of an indazole moiety (Figure 1). AB-PINACA is structurally related to AKB-48 (APINACA), but contains a 1-amino-3-methyl-1-oxobutan-2-yl substituent instead of the adamantyl group in AKB-48. They were first reported in Japan in 2013.[12] Recently, in a period of roughly a month, 76 cases of suspected intoxications were reported by emergency departments in hospitals in Colorado.[13] The patients, primarily young men, presented with altered mental status, tachycardia, and seizures. In mixtures claimed to be ingested by the patients, ADB-PINACA, a compound closely related to AB-PINACA with the only difference being an extra methyl group in ADB-PINACA, was consistently identified.

Knowledge of the pharmacology of synthetic cannabimimetic agents is limited. Some have been assayed for binding affinity to cannabinoid receptors. For example, AB-FUBINACA was found to bind to CB_1 with a K_i of 0.9 nM,[14] which is 10-fold greater than for the well-known cannabinoid receptor agonist JWH-018.[15]

Wohlfarth *et al.* demonstrated using human hepatocytes that the major metabolic transformation of PB-22 and its fluorinated analogue 5F-PB-22 was hydrolysis of the ester bond.[16] However, they did not investigate which specific enzymes were involved in the metabolism of these compounds, and the closely related compound, BB-22, was not included in their studies.

Recently, Takayama *et al.* studied the metabolism of AB-PINACA, AB-FUBINACA, ADB-FUBINACA, PB-22 and 5F-PB-22 using human liver microsomes.[17] However, their study was rather limited, in that only a single metabolite was identified for PB-22, 5F-PB-22, and AB-FUBINACA, and three metabolites for AB-PINACA. This is in strong contrast to Wohlfarth *et al.*, who identified a total of 20 and 22 metabolites for PB-22 and 5F-PB-22, respectively.[16]

Preliminary investigations of the metabolism of AB-PINACA and AB-FUBINACA by our group identified amide hydrolysis as a major metabolic pathway. This pathway was found to be NADPH-independent suggesting no involvement of cytochrome P450 (CYP) enzymes. Thus, like the quinolineindoles, the indazole carboxamide derivatives seem to be susceptible to hydrolytic biotransformations. It is therefore likely, that esterases are involved in the metabolism of these compounds.

To date, several esterases involved in xenobiotic metabolism have been identified.[18] The most studied are butyrylcholinesterase (BChE), as well as carboxylesterase 1 (CES1) and 2 (CES2). BChE is synthesized in the liver and secreted into plasma, and has been found to metabolize drugs such as succinylcholine, bambuterol and cocaine.[19–21] The carboxylesterases are found in many tissues, with CES1 being most abundant in the liver and lung, and CES2 in the intestinal wall.[22] CES1 is involved in the metabolism of a range of pharmaceuticals and drugs of abuse, some of which are methylphenidate, pethidine, cocaine, oseltamivir, clopidogrel, rufinamide, dabigatran etexilate, and several ester-containing ACE-inhibitors such as enalapril, ramipril and trandolapril.[23–29] CES2 has been implicated in the metabolism of compounds such as irinotecan, prasugrel and flutamide.[30–32] Other drug-metabolizing esterases include arylacetamide deacetylase (AADAC), found to hydrolyze, for example phenacetin and rifamycin antibiotics,[33,34] and paraoxonases (PON), found to hydrolyze, for example, lactone-containing statins.[35]

Several esterases, including CES1, BChE, and PON1, have been found to exhibit polymorphism, leading to variations in the kinetics of substrates.[36–38] Thus, to be better able to predict toxic potential of drugs and interpret toxicological results, it can be of value to identify the esterase(s) involved in the metabolism of a given drug.

In the present study, we sought to fully characterize the phase I metabolism of AB-PINACA and AB-FUBINACA in human liver microsomes. Additionally, identification of the human esterase(s) responsible for the major metabolic pathway of PB-22 and 5F-PB-22 was

performed. The results presented can be utilized in the development of analytical methods in clinical and forensic work, as well as advance our understanding of xenobiotic metabolism by esterases.

Materials and methods

Chemicals, reagents, and reference compounds

p-nitrophenyl acetate (PNPA), acetylthiocholine iodide (ATCI), butyrylthiocholine iodide (BTCI), 5,5′-dithiobis(2-nitrobenzoic acid) (DTNB), paraoxon, tetraisopropyl pyrophosphoramide (iso-OMPA), 4-(hydroxymercuri)benzoic acid sodium (4-HMB) and physostigmine were from Sigma-Aldrich (St Louis, MO, USA); *p*-nitrophenol (PNP) was from Fluka (Buchs, Switzerland); BB-22, PB-22, 5F-PB-22, cyclohexylmethylindole-3-carboxylic acid (CHMI-COOH), pentylindole-3-carboxylic acid (PI-COOH), 5-fluoro-pentylindole-3-carboxylic acid (5F-PI-COOH) and JWH-200 were from Cayman Chemical (Ann Arbor, MI, USA); AB-PINACA, (1-pentyl-1*H*-indazole-3-carbonyl)-L-valine (AB-PINACA-COOH), AB-FUBINACA, (1-(4-fluorobenzyl)-1*H*-indazole-3-carbonyl)-L-valine (AB-FUBINACA-COOH), JWH-018-N-carboxy and JWH-018-N-carboxy-d4 were from Chiron (Trondheim, Norway). Unless otherwise stated, phosphate buffer (100 mM, pH 7.4) was used for all enzyme assays and was produced from potassium phosphate and dipotassium phosphate (both from Merck, Darmstadt, Germany). HEPES buffer (100 mM, pH 7.4) was produced from HEPES and HEPES sodium salt (both from Sigma-Aldrich). Other solvents and chemicals were commercially available and of analytical or liquid chromatography-mass spectrometry (LC-MS) grade.

Biological materials

Pooled human liver microsomes (HLM), recombinant human CES1 (CES1b/CES1A1), and CES2 (prepared from baculovirus-infected High-Five insect cells) were obtained from BD Gentest (Woburn, MA, USA). Insect cell microsomes from wild-type baculovirus-infected cells (product no. 456200) and NADPH regenerating system solution A and B (product nos 451220 and 451200) were from Corning Inc. (Corning, NY, USA). Pooled human pulmonary microsomes (from smokers) were from XenoTech, LLC (Lenexa, KS, USA).

Human serum from six donors (three males and three females) was acquired from the blood bank at Copenhagen University Hospital. The serum was pooled and stored at −80 °C. Protein concentration in the pooled serum was determined by the Bradford method using a Protein Quantification Kit-Rapid from Sigma-Aldrich (St Louis, MO, USA). The protein content was 56.8 ± 5 mg/mL (n = 4).

Esterase activities in human serum

AChE and BChE activities in pooled human serum were determined in quadruplicate by using acetylthiocholine iodide and butyrylthiocholine iodide as substrates, respectively. In both cases, the thiocholine produced reacts with DTNB (Ellman's reagent) to produce the yellow-colored 5-thio-2-nitrobenzoate (DTA).[39] Iso-OMPA was used as selective BChE inhibitor when determining AChE activity.[40] Pooled serum diluted to 250 μg protein/mL for AChE and 125 μg protein/mL for BChE was incubated with 2 mM DTNB (and for AChE with 0.1 mM iso-OMPA) for 15 min at 37 °C. Then 0.5 mM of the corresponding substrate was added and the formation of DTA monitored at 405 nm for 20 min at 2-min intervals using a Sunrise microplate reader (Tecan, Grödig, Austria). Enzyme activities were calculated using a molar absorption coefficient for DTA of 13,680 M^{-1} cm^{-1}.[41]

PON activity in pooled human serum was determined in quadruplicate by using paraoxon as substrate. Pooled serum diluted to 500 μg protein/mL was incubated at 37 °C with 5 mM paraoxon in 100 mM HEPES buffer pH 7.4 containing 2 mM $CaCl_2$. The formation of PNP was monitored at 405 nm for 30 min at 2-min intervals using a Sunrise microplate reader. Quantification was conducted using a calibration curve obtained from standard samples of PNP (10–500 μM) prepared in the assay conditions.

Metabolite identification

Metabolites of AB-PINACA and AB-FUBINACA were identified by incubation in HLM. One mM stock solutions of the two compounds were prepared in methanol and used for the incubations. Five μM of each compound was incubated in phosphate buffer in a total volume of 250 μL with 1 mg protein/mL HLM, 1.3 mM NADP+, 3.3 mM glucose-6-phosphate, 3.3 mM $MgCl_2$, 0.4 U/mL glucose-6-phosphate dehydrogenase, and 0.05 mM sodium citrate. The temperature was kept at 37 °C during the incubation. The reaction was initiated by the addition of the NADPH regenerating system (solution A and B). At time points 0, 5, 10, 15, 20, 30, 60, 90, 120, and 180 min, 20 μL aliquots of the incubation were transferred to 40 μL ice-cold methanol containing an internal standard (JWH-018-N-carboxy-d4). Incubations without NADPH regenerating system (solution A and B) served as negative controls.

Metabolites were detected using a high-resolution accurate-mass mass spectrometer system. The system consisted of a Q-Exactive mass spectrometer (Thermo Scientific, Bremen, Germany) interfaced to a Dionex Ultimate 3000 UHPLC system (Thermo Scientific, Bremen, Germany). Chromatographic separation was performed on a Kinetex 2.6 μm Phenyl-hexyl 100 Å column (50 mm x 2.1 mm) (Phenomenex, Torrance, CA, USA), which was maintained at a temperature of 40 °C. The mobile phase was composed of solvents A (water with 0.1% formic acid) and B (methanol with 0.1% formic acid) delivered at a flow rate of 0.3 mL/min. The gradient had a total run-time of 10 min starting at 35 % B for 0.5 min, increasing to 60 % B over 5.5 min, increasing to 90 % over 1 min, isocratic for 1 min before re-equilibration for 2.5 min. The injection volume was 5 μL.

The Q-Exactive was operated with positive electrospray ionization (ESI+) in data-dependent acquisition (DDA) mode with MS/MS scans of the eight most intense ions following each full scan. Full scan data were collected in profile mode from *m/z* 200–800 at a resolution of 70 000 (FWHM at *m/z* = 200), while the MS/MS spectra were acquired at a lower resolution of 17 500 using a normalized collision energy of 40 eV. Nitrogen was used as the collision gas.

The Q-Exactive was externally calibrated in positive and negative mode twice a week using Pierce® ESI calibration solutions (Thermo Scientific, Bremen, Germany).

The Q-Exactive was controlled by TraceFinder 3.1 (Thermo Scientific, Bremen, Germany). Metabolites were entered into a TraceFinder processing method with identification based on absolute area, exact mass, and at least one fragment present for each analyte. The mass error in the MS and MS/MS scans were set to 2.5 and 7 ppm, respectively, based on the long-term accuracies measured on a system control mixture.

Product ions were used as diagnostic ions to identify metabolites and to assign the placement of metabolic transformations, as it is assumed metabolites have similar fragmentation patterns as their parent compounds. Retention times were subsequently added to distinguish the different isomeric metabolites identified. Xcalibur

(Thermo Scientific, Bremen, Germany) was used to examine the extracted ion chromatograms (EICs) and MS/MS spectra in order to further refine the TraceFinder processing method.

Incubation with recombinant esterases and human serum

The hydrolysis of BB-22, PB-22, 5F-PB-22, AB-PINACA, and AB-FUBINACA by recombinant human CES1 and CES2, as well as pooled human serum, was investigated. Substrate (10 μM) was incubated for 20 min at 37 °C with a final protein concentration of recombinant enzyme of 50 μg/mL for BB-22, PB-22, and 5F-PB-22, and 100 μg/mL for AB-PINACA and AB-FUBINACA. Final protein concentration for serum was 500 μg/mL. The final volume of incubations was 100 μL. Incubations with serum were conducted in 100 mM HEPES buffer with 2 mM $CaCl_2$. All incubations were performed in quadruplicate and negative controls were included in which substrates were incubated with microsomes from the wild-type baculovirus-infected insect cells at the same protein concentrations as the recombinant insect microsomes. Sampling was performed after 0, 10, and 20 min by transferring aliquots of 20 μL to an equal volume of cold acetonitrile with 0.5% formic acid and 2 ng/mL internal standard JWH-018-N-carboxy for BB-22, PB-22, and 5F-PB-22 or 4 ng/mL JWH-200 for AB-PINACA and AB-FUBINACA. Next, 110 μL of 0.1% formic acid in water was added, and the samples were centrifuged at 2000 × *g*, 5 °C, for 10 min. Formation of hydrolytic products was quantified as described in the analytical methods section below. Hydrolysis rates were corrected for spontaneous hydrolysis, i.e., non-enzymatic hydrolysis, by subtracting any product formed in the negative controls. Final concentration of DMSO was 1% in all incubations, which has previously been shown to be well tolerated by carboxylesterases.[42]

Esterase inhibition assay

The effect of a panel of selective esterase inhibitors on PB-22 and AB-PINACA hydrolysis by HLM and HPM was evaluated using benzil, loperamide, 4-HMB, and physostigmine. Inhibitors at final concentrations of 1, 10, and 100 μM were pre-incubated with HLM and HPM (200 μg protein/mL) for 5 min at 37 °C. Reactions were initiated by adding substrate at a final concentration of 5 μM. The final incubation volume was 100 μL. Reactions were stopped after 15 min for AB-PINACA and 20 min for PB-22 as described in the previous section. All incubations were performed in triplicate and positive control incubations in the absence of inhibitor were also included. The final concentration of DMSO was 1.5 % in all incubations, including the controls. Formation of hydrolytic products was quantified as described in the analytical methods section below. The effect of inhibitors was calculated by comparing the response (analyte peak area divided by internal standard peak area) of the hydrolytic product in an incubation containing inhibitor with that of the positive controls.

Analytical methods

CHMI-COOH, PI-COOH, 5F-PI-COOH, AB-PINACA-COOH, and AB-FUBINACA-COOH were quantified with UPLC-MS/MS. Chromatographic separation was performed with an ACQUITY UPLC I-Class system (Waters Corporation, Milford, MA, USA). The system consisted of a binary solvent manager, a column manager, a flow-through needle sample manager, a sample organizer and an Xevo TQ-S mass spectrometer. An ACQUITY UPLC HSS T3 column (1.8 μm, 2.1 × 100 mm) from Waters was used for separation. Isocratic chromatographic methods were developed to separate the parent compounds from their respective hydrolytic metabolites. The mobile phase consisted of 0.1% formic acid in water and methanol for all analytes. For CHMI-COOH, 5F-PI-COOH and PI-COOH, the composition was (15:85, *v/v*), while it was (30:70, *v/v*) for AB-FUBINACA-COOH, and (20:80, *v/v*) for AB-PINACA-COOH. The runtime was 2 min for all methods. Flow rate was 0.4 mL/min, column temperature 50°C and injection volume 1 μL for all methods.

Data were acquired in positive electrospray ionization mode with Masslynx 4.1 software (Waters Corporation, Milford, MA, USA). Multiple reaction monitoring (MRM) was used for data collection. Monitored mass transitions were *m/z* 258.15 > 144.04, *m/z* 232.13 > 144.04, *m/z* 250.12 > 144.04, *m/z* 370.2 > 253.1, and *m/z* 332.2 > 215.1 for CHMI-COOH, PI-COOH, 5F-PI-COOH, AB-FUBINACA-COOH and AB-PINACA-COOH, respectively. Mass transitions for the internal standards were *m/z* 372.16 > 155.05 and *m/z* 385.19 > 155.05 for JWH-018-N-carboxy and JWH-200, respectively. Cone voltage and collision energy of 20 V and 20 eV, respectively,

Table 1. Metabolites of AB-PINACA after incubation with human liver microsomes

Peak ID	Proposed modification	RT (min)	Elemental composition	Precursor $[M+H]^+$ (*m/z*)	Product ions (*m/z*)[§]	With NADPH	Without NADPH
M1	Hydrolysis (amide, distal)	7.44	$C_{18}H_{25}N_3O_3$	332.1969	145, 215, 286	Present	Present
M2	Mono-hydroxylation (pentyl moiety) of M1	5.11	$C_{18}H_{25}N_3O_4$	348.1918	145, 231, 302	Present	Absent
M3	Mono-hydroxylation (pentyl moiety) of M1	5.43	$C_{18}H_{25}N_3O_4$	348.1918	145, 231, 302	Present	Absent
M4	Mono-hydroxylation (indazole moiety) of M1	7.06	$C_{18}H_{25}N_3O_4$	348.1918	161, 231, 302	Present	Absent
M5	Mono-hydroxylation (pentyl moiety)	4.09	$C_{18}H_{26}N_4O_3$	347.2078	145, 231, 302	Present	Absent
M6	Mono-hydroxylation (pentyl moiety)	4.48	$C_{18}H_{26}N_4O_3$	347.2078	145, 231, 302	Present	Absent
M7	Mono-hydroxylation (indazole moiety)	6.29	$C_{18}H_{26}N_4O_3$	347.2078	161, 231, 302	Present	Absent
M8	Mono-hydroxylation (1-amino-3-methyl-1-oxobutane moiety)	6.38	$C_{18}H_{26}N_4O_3$	347.2078	145, 215, 302	Present	Absent
M9	Di-hydroxylation (1-amino-3-methyl-1-oxobutane + pentyl moiety)	2.58-2.85	$C_{18}H_{26}N_4O_4$	363.2027	145, 231, 318	Present	Absent
M10	Di-hydroxylation (1-amino-3-methyl-1-oxobutane + pentyl/indazole moiety)	3.19	$C_{18}H_{26}N_4O_4$	363.2027	231, 318	Present	Absent
P	AB-PINACA	7.22	$C_{18}H_{26}N_4O_2$	331.2129	145, 215, 286	-	-

[§] Product ions are shown with nominal masses to conserve space.

was applied for all analytes. Other MS parameters were: Capillary voltage 1 kV, source temperature 150 °C, desolvation temperature 500 °C, cone gas flow 150 L/h, and desolvation gas flow 800 L/h. Argon was used as collision gas. The measuring range was 0.1 to 10 μM for all analytes.

Results and discussion

Esterase activities in pooled human serum

The activities of AChE, BChE, and PON were determined in pooled human serum using selective substrates. The activities (n = 4) were 0.475 and 60.6 nmol thiocholine/min/mg protein for AChE and BChE, respectively. The PON activity (n = 4) was 5.93 nmol *p*-nitrophenol/min/mg protein. The results demonstrate the presence and activity of these enzymes, and verify the suitability of this matrix as a source of plasma esterases.

Incubation of AB-PINACA with HLM

Phase I metabolism of AB-PINACA was investigated by incubation in mixtures containing HLM with and without NADPH-regenerating system. An overview with retention times and *m/z*-values of precursor and product ions for parent compound and any identified metabolites is given in Table 1. MS/MS spectrum for AB-PINACA is shown in Figure 2 and formation of metabolites over time is shown in Figure 3. EICs and MS/MS spectra for all identified metabolites are given in the supplementary material.

Fragmentation of AB-PINACA resulted in three observed product ions with *m/z* 145, 215, and 286 which would be consistent with the indazole-3-carbaldehyde moiety without and with the pentyl side-chain, and the precursor ion without the distal methanamide, respectively (Figure 2).

Interestingly, a depletion of AB-PINACA in the incubation without NADPH was observed (Figure 3B). In this incubation, the formation of a single species (M1) was observed with a slightly increased retention time of 7.44 min and an *m/z*-value one unit higher than the parent compound. The MS/MS spectrum of this metabolite revealed identical product ions as the parent compound. This is consistent with M1 being the product of hydrolysis of the distal amide. M1 was not observed in the absence of HLM (data not shown), indicating that M1 is the result of a NADPH-independent enzymatic reaction. The identity of M1 was verified to be AB-PINACA-COOH by injection of a synthesized reference standard (Supplementary Material).

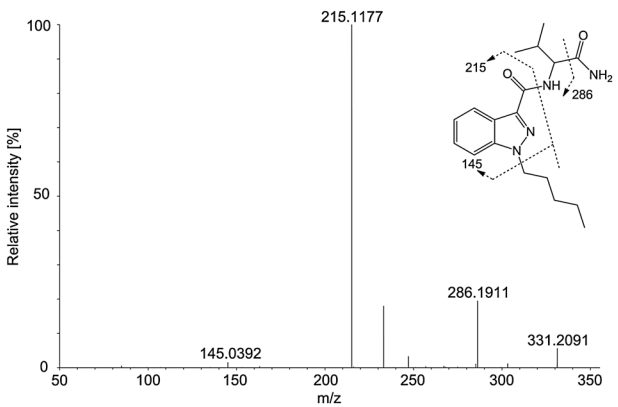

Figure 2. MS/MS spectrum for AB-PINACA with proposed structures of product ions.

After incubation for three hours in the presence of NADPH, multiple metabolites were observed: Hydrolysis to AB-PINACA-COOH (M1), mono-hydroxylations (M5-M8), di-hydroxylations (M9-M10), and further mono-hydroxylations of AB-PINACA-COOH (M2-M4). The hydroxylated metabolites suggest a role for the CYP-system in the metabolism of AB-PINACA. The proposed metabolic pathway for AB-PINACA is shown in Figure 4.

Four mono-hydroxylated products of AB-PINACA were identified (M5–M8); one major metabolite (M5), and three minor metabolites (M6, M7, and M8, respectively). MS/MS spectra of metabolites M5 and M6 contained product ions at *m/z* 145, 231 and 302, indicating a hydroxylation on the pentyl side-chain. The MS/MS spectrum of M7 contained product ions at *m/z* 161, 231, and 302 indicating a hydroxylation at the indazole moiety, while the product ions of M8 at *m/z* 145, 215, and 302 suggest a hydroxylation at the 1-amino-3-methyl-1-oxobutane moiety. The peaks of M7 and M8 were not completely separated, but clearly contained different species. The mono-hydroxylated metabolites were rapidly formed (Figure 3A); a depletion of M8 was observed after 30 min of incubation, indicating further transformation of this metabolite. A depletion of M5 and M6 was only observed after 120 min of incubation, suggesting that these two metabolites are less prone to undergo further metabolism.

Two di-hydroxylated products of AB-PINACA were identified; both minor metabolites (M9 and M10, respectively). The MS/MS spectra for both metabolites contain product ions at *m/z* 231 and 318, indicating one hydroxylation at the 1-amino-3-methyl-1-oxobutane moiety and another at the indazole/pentyl moiety. M9 had an additional product ion of *m/z* 145, isolating the second

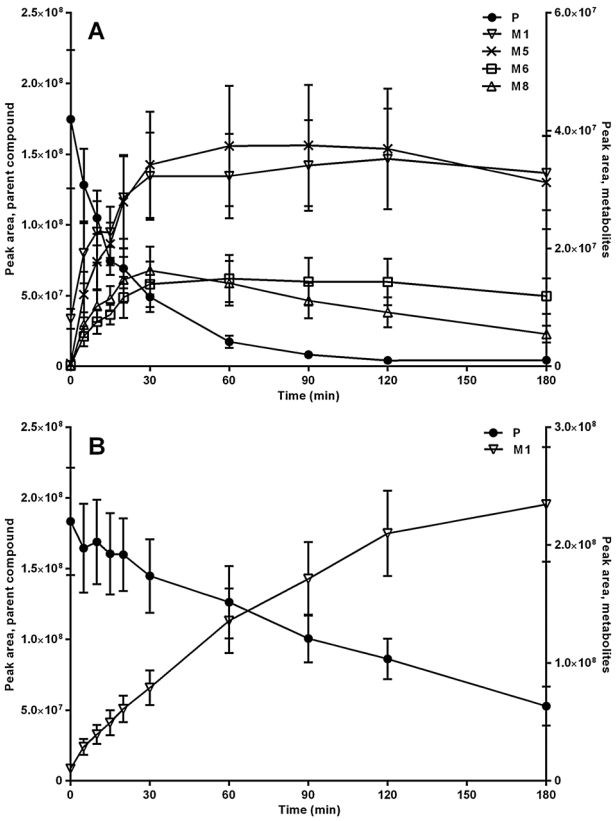

Figure 3. Formation of metabolites of AB-PINACA after incubation in HLM with (A) and without (B) NADPH regeneration system. For clarity, minor metabolites are omitted. Values represent mean ± S.E.M. (n = 3). The peak area of the parent compound is shown on the left y-axis, while the peak area of metabolites is shown on the right y-axis.

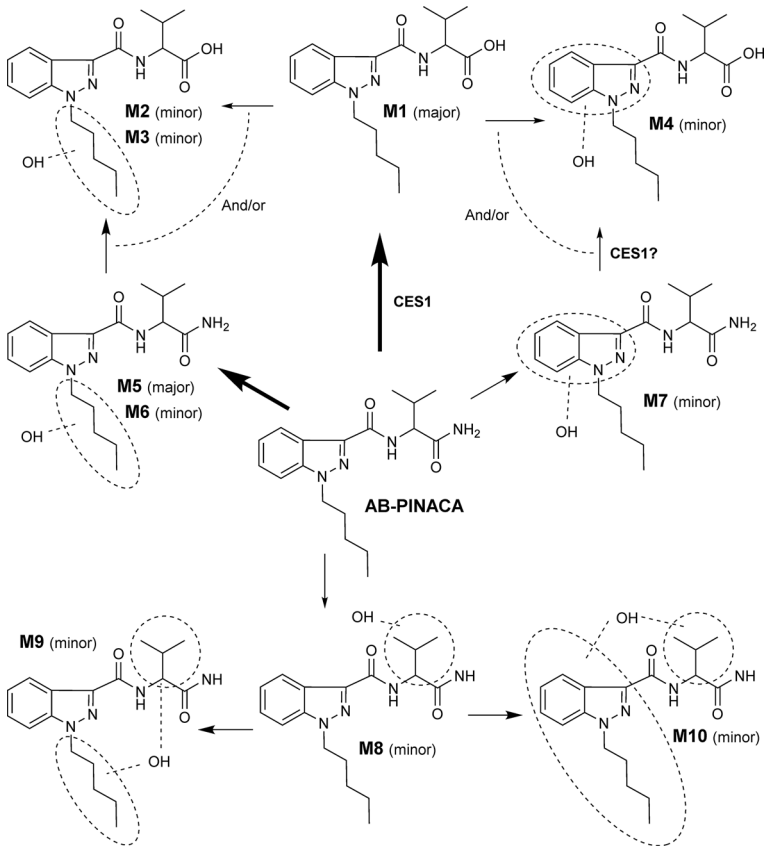

Figure 4. Proposed phase I metabolic pathways of AB-PINACA in human liver microsomes. Major pathways are indicated by thick arrows. M1 = AB-PINACA-COOH.

hydroxylation site to the pentyl side-chain. The MS/MS spectrum for M10 contains neither the product ion for the native indazole moiety (*m/z* 145) nor the product ion for the indazole with a hydroxylation (*m/z* 161). It was therefore not possible to narrow down the location of the second hydroxy group for M10. Di-hydroxylated products were observed after 20 min of incubation. M9 and M10 were both formed concomitantly with the depletion of the mono-hydroxylated metabolite M8, indicating that the di-hydroxylated metabolites are generated as a result of further metabolism of M8. The peak of M9 was broad and appeared to be two overlapping peaks. This is likely caused by two co-eluting di-hydroxylated metabolites, corresponding to hydroxylations of two different carbon atoms in the N-pentyl chain.

M1 was observed in both the incubation with and without NADPH (Figure 3), and is likely to be a major metabolite of AB-PINACA *in vivo*. In the absence of NADPH, formation of M1 was rapid and continued throughout the incubation, whereas the formation of this metabolite in the presence of NAPDH was initially rapid, but did not reach the same levels as in the absence of NADPH. This suggests that M1 could be a substrate for CYP-enzymes. Indeed, three mono-hydroxylated products of AB-PINACA-COOH were observed (M2, M3, and M4, respectively). These transformations were parallel to the parent compound with M2 and M3 being hydroxylated at the N-pentyl side-chain, and M4 hydroxylated at the indazole moiety.

Takayama et al. also investigated the metabolism of AB-PINACA using incubations in HLM.[17] They only identified three mono-hydroxylated metabolites, corresponding to the three most abundant hydroxylated metabolites (M5, M6, and M8) observed in our study. However, Takayama *et al.* failed to detect the major metabolite M1, as well as several minor hydroxylated metabolites. Takayama *et al.* employed a mass spectrometer not capable of exact-mass measurements and were thus unable to utilize mass-defect filtering. They did not state how their software filters were designed, and it is therefore possible that the software flagged the peak of M1 as an unlikely metabolite.

Additionally, the transformation of a primary amide to a carboxylic acid only causes an increase of 1 Da in mass, which can, if co-elution of the peaks occurs, easily be overlooked and perhaps wrongly assigned as an isotope in the mass spectrum. However, in our chromatography the peaks of AB-PINACA and M1 were baseline-separated, and considering the chromatography used by Takayama *et al.* was quite comparable, co-elution is unlikely to have occurred. These findings emphasize the need of manual examination of results when employing software solutions that provide automated detection and assignment of metabolites.

Incubation of AB-FUBINACA with HLM

Like for AB-PINACA, the phase I metabolism of AB-FUBINACA was investigated by incubation in HLM with and without the NADPH-regenerating system. An overview with retention times and *m/z*-values of precursor and product ions for AB-FUBINACA and any identified metabolites is given in Table 2. MS/MS spectrum for AB-FUBINACA is shown in Figure 5 and formation of metabolites over time is shown in Figure 6. EICs and MS/MS spectra for all identified metabolites are given in the supplementary material.

Fragmentation of AB-FUBINACA resulted in three observed product ions at *m/z* 109, 253, and 324 most likely corresponding to 4-fluorobenzyl, the indazole-3-carbaldehyde moiety with the

Table 2. Metabolites of AB-FUBINACA after incubation with human liver microsomes

Peak ID	Proposed modification	RT (min)	Elemental composition	Precursor $[M+H]^+$ (*m/z*)	Product ions (*m/z*)[§]	With NADPH	Without NADPH
M1	Hydrolysis (amide, distal)	7.30	$C_{20}H_{20}FN_3O_3$	370.1561	109, 253, 324	Present	Present
M2	Mono-hydroxylation (1-amino-3-methyl-1-oxobutane moiety) of M1	6.23	$C_{20}H_{21}FN_3O_4$	386.1511	109, 253, 340	Present	Absent
M3	Mono-hydroxylation (indazole moiety) of M1	6.82	$C_{20}H_{21}FN_3O_4$	386.1511	109, 269, 340	Present	Absent
M4	Mono-hydroxylation (1-amino-3-methyl-1-oxobutane moiety)	5.83	$C_{20}H_{21}FN_4O_3$	385.1670	109, 253, 340	Present	Absent
M5	Di-hydroxylation (indazole + 1-amino-3-methyl-1-oxobutane moiety) of M1	4.78	$C_{20}H_{21}FN_3O_5$	402.1460	109, 269	Present	Absent
M6	Di-hydroxylation (indazole + 1-amino-3-methyl-1-oxobutane moiety)	4.35	$C_{20}H_{21}FN_4O_4$	401.1620	109, 269, 356	Present	Absent
M7	Di-hydroxylation (1-amino-3-methyl-1-oxobutane moiety)	5.30	$C_{20}H_{21}FN_4O_4$	401.1620	109, 253	Present	Absent
P	AB-FUBINACA	6.99	$C_{20}H_{21}FN_4O_2$	369.1721	109, 253, 324	-	-

[§] Product ions are shown with nominal mass to conserve space.

4-fluorobenzyl group and the precursor ion without the methanamide, respectively.

The pattern of metabolism was similar to that of AB-PINACA and is shown in Figure 7. As for AB-PINACA, hydrolysis of the distal amide resulted in a major metabolite M1. As shown in Figure 6B, the generation of M1 was independent of NAPDH. The identity of M1 as AB-FUBINACA-COOH was confirmed by injection of a reference standard (Supplementary Material).

Due to replacement of the pentyl chain in AB-PINACA with a 4-fluorobenzyl group in AB-FUBINACA, alternative sites of hydroxylation dominated. The primary site of hydroxylation was the 1-amino-3-methyl-1-oxobutane moiety, resulting in a major mono-hydroxylated metabolite (M4). No hydroxylations were observed in the 4-fluorobenzyl moiety.

Two minor di-hydroxylated metabolites were identified (M6 and M7). MS/MS spectra for both di-hydroxylated products contain a product ion at *m/z* 109, indicating that no transformation is occurring in the 4-fluorobenzyl moiety. M7, the more abundant of the two metabolites, additionally had a product ion at *m/z* 253, indicating that both hydroxylations are located in the 1-amino-3-methyl-1-oxobutane moiety. M6 had two additional product ions at *m/z* 269 and 356, indicating one hydroxylation at the indazole moiety and one at the 1-amino-3-methyl-1-oxobutane moiety.

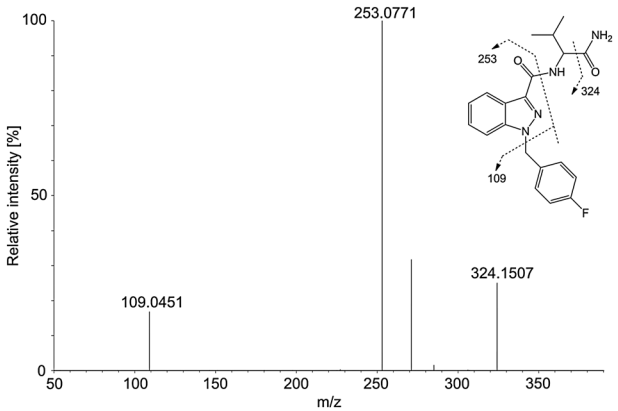

Figure 5. MS/MS spectrum for AB-FUBINACA with proposed structures of product ions.

As for AB-PINACA, further transformations of M1 were observed. Two minor metabolites (M2 and M3) were identified as further mono-hydroxylations of M1. The MS/MS spectrum of M2, the more abundant of the two, contained product ions at *m/z* 109, 253, and 340, indicating a hydroxylation at the 1-amino-3-methyl-1-oxobutane moiety, while the product ions of M3 at *m/z* 109, 269, and 340 suggested a hydroxylation at the indazole moiety.

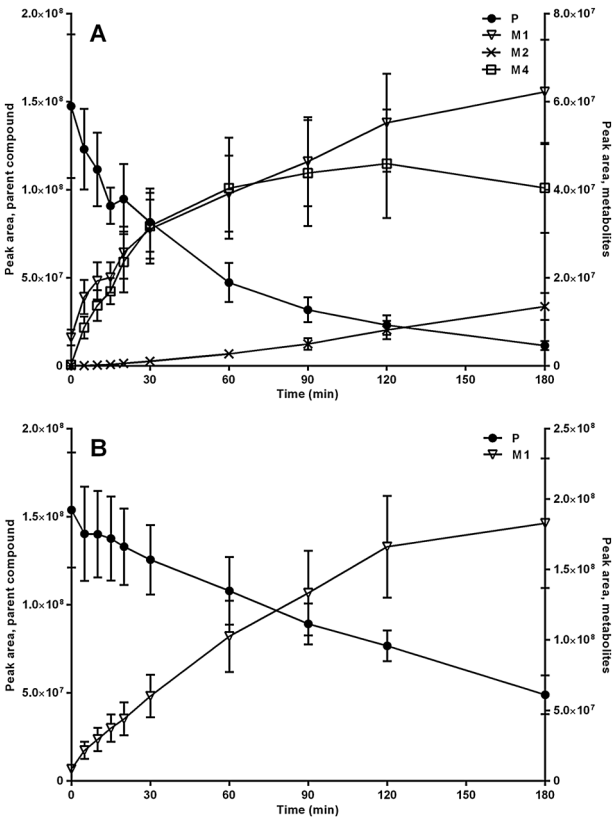

Figure 6. Formation of metabolites of AB-FUBINACA after incubation in HLM with (A) and without (B) NADPH regeneration system. For clarity, minor metabolites are omitted. Values represent mean ± S.E.M. (n = 3). The peak area of the parent compound is shown on the left y-axis, while the peak area of metabolites is shown on the right y-axis.

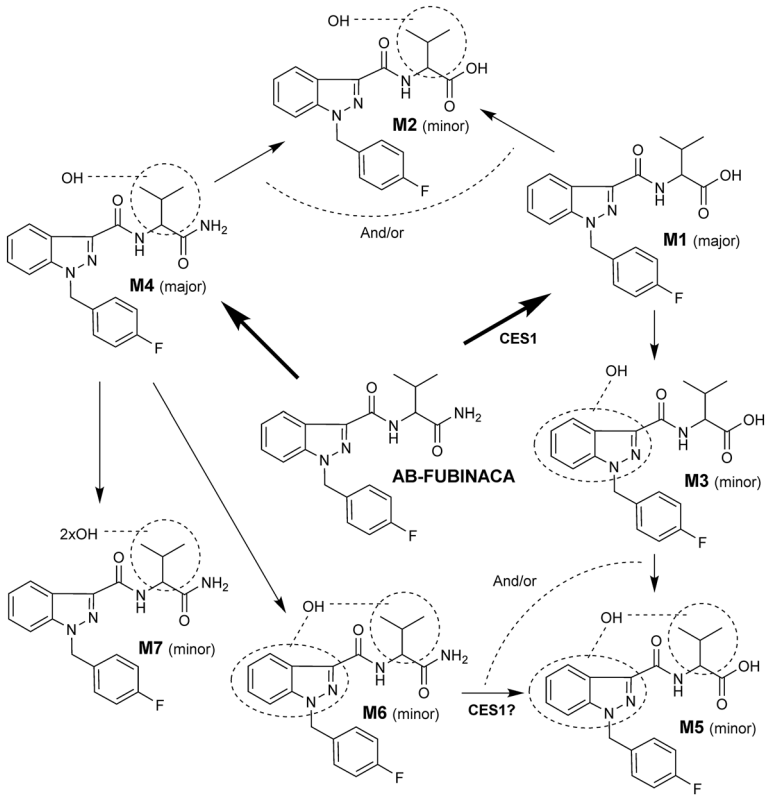

Figure 7. Proposed phase I metabolic pathways of AB-FUBINACA in humans. Major pathways are indicated by thick arrows. M1 = AB-FUBINACA-COOH.

Additionally, a di-hydroxylation of M1 was identified as a minor metabolite after 30 minutes of incubation (M5). The MS/MS spectrum of M5 contained product ions at *m/z* 109 and 269 indicating one hydroxylation at the indazole moiety and the other at the 1-amino-3-methyl-1-oxobutane moiety.

Takayama *et al.* only identified a single metabolite of AB-FUBINACA, corresponding to the only mono-hydroxylated metabolite M4 found in the present study, and thus missed the major hydrolyzed metabolite M1 and all the minor metabolites.[17]

Incubation of AB-PINACA and AB-FUBINACA with recombinant CES1, CES2, and human serum

To identify the enzymes(s) responsible for the hydrolysis of the primary amide in AB-PINACA and AB-FUBINACA, the two compounds were incubated with recombinant human CES1 and CES2, as well as pooled human serum. The results are shown in Figure 8. Both compounds were hydrolyzed by both CES1 and CES2. CES1 demonstrated 4.6-fold and 3.5-fold higher hydrolytic activity than CES2 for AB-PINACA and AB-FUBINACA, respectively. Few examples of amide hydrolysis by carboxylesterases have been demonstrated previously. Williams *et al.* found that both CES1 and CES2 could hydrolyze rufinamide, with CES1 having roughly 3.8-fold higher activity than CES2.[26] Like for AB-PINACA and AB-FUBINACA, it is a primary amide in rufinamide that is hydrolyzed.

No hydrolytic activity towards AB-PINACA and AB-FUBINACA was detected in human serum. This indicates that esterases found in human serum, such as AChE, BChE, and PON, are not capable of metabolizing these compounds. Furthermore, no hydrolysis could be detected in the negative controls after 20 min, suggesting that the compounds are relatively stable at physiological pH and that non-enzymatic hydrolysis in vivo is unlikely.

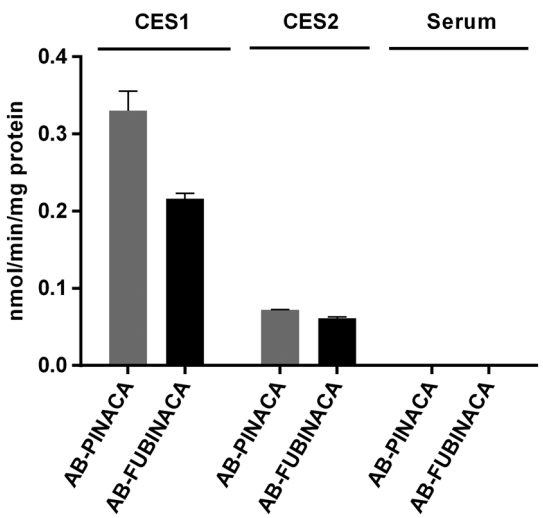

Figure 8. Incubation of 10 μM AB-PINACA and AB-FUBINACA with recombinant CES1, CES2 and pooled human serum at 37°C for 20 min. Formed hydrolytic products, AB-PINACA-COOH and AB-FUBINACA-COOH, respectively, were quantified and normalized by time and protein contents. Values represent mean ± S.E.M. (n = 4).

Incubation of BB-22, PB-22, and 5F-PB-22 with recombinant CES1, CES2, and human serum

BB-22, PB-22, and 5F-PB-22 were incubated with recombinant human CES1 and CES2, as well as pooled human serum. The

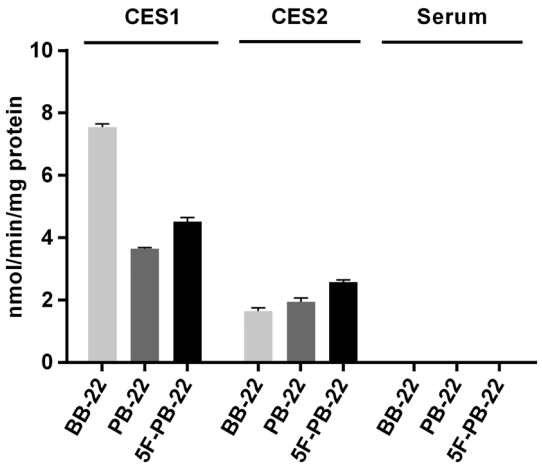

Figure 9. Incubation of 10 μM BB-22, PB-22 and 5F-PB-22 with recombinant CES1, CES2 and pooled human serum at 37°C for 10 min. Formed corresponding hydrolytic products were quantified and normalized by time and protein contents. Values represent mean ± S.E.M. (n = 4).

results are shown in Figure 9. All three compounds were hydrolyzed by both CES1 and CES2. The activity of CES1 was roughly 2- to 5-fold higher than for CES2 for the three compounds. As for AB-PINACA and AB-FUBINACA, no hydrolytic activity was detected in human serum, ruling out contributions from plasma esterases, such as AChE, BChE and PON. Furthermore, no hydrolysis could be detected in negative controls after 20 min, suggesting stability at physiological pH and non-enzymatic hydrolysis *in vivo* to be unlikely.

Inhibition of AB-PINACA hydrolysis in HLM and HPM

The effect of four known esterase inhibitors on the hydrolysis of AB-PINACA to AB-PINACA-COOH (M1) in HLM and HPM was studied. Due to smoking being a common administration route for cannabis as well as synthetic cannabinoids, a certain amount of these compounds can be expected to be metabolized in lung tissue. Therefore, we included pulmonary microsomes in our inhibition study in addition to liver microsomes. The results are shown in Figure 10.

Benzil, which is a selective carboxylesterase inhibitor,[43] was the only compound tested to potently inhibit AB-PINACA hydrolysis. In both HLM and HPM, the hydrolysis was completely abolished at 100 μM benzil, while there was less than 10% remaining activity at 10 μM benzil. Loperamide, a selective CES2 inhibitor,[44] exhibited a minor concentration-dependent inhibition with roughly 80% remaining activity at 100 μM. This is consistent with CES2 having lower activity than CES1 towards AB-PINACA hydrolysis and also having lower expression in both liver and lung. 4-HMB, a sulfhydryl-reacting agent and inhibitor of cysteine-dependent enzymes such as PONs,[45] displayed no significant inhibition of AB-PINACA hydrolysis. Instead a slight increase in hydrolytic activity at 10 and 100 μM 4-HMB was observed. This increase in activity was unexpected, but is consistent with what Williams *et al*. found for rufinamide at higher concentrations of 4-HMB and 4-chloromercurybenzoic acid (PCMB), a closely related sulfhydryl-reacting agent.[26] In both HLM and HPM, there was a minor inhibition by physostigmine at 100 μM.

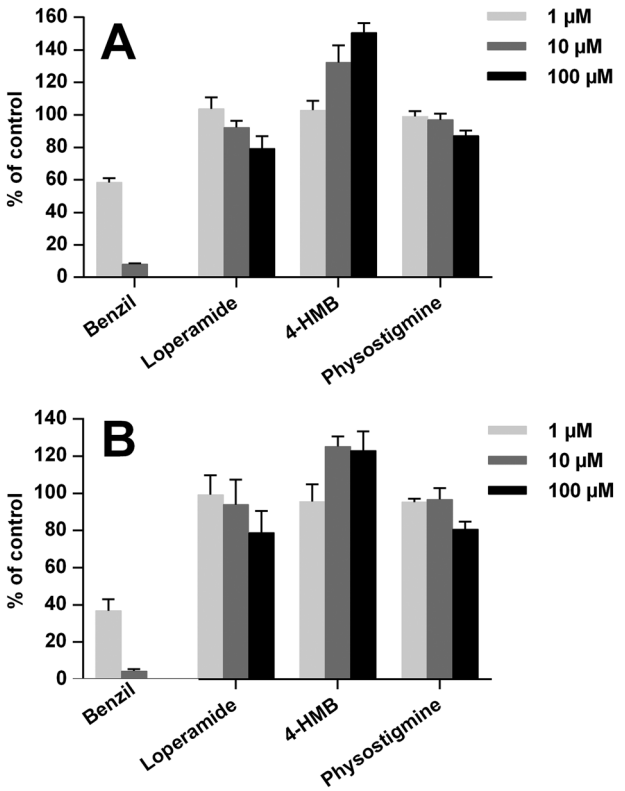

Figure 10. Effect of different selective chemical esterase inhibitors on the hydrolysis of AB-PINACA in HLM (A) and HPM (B). 5 μM substrate was added after 5 min preincubation of 1, 10 or 100 μM inhibitor with 200 μg/mL HLM or HPM. Reactions were stopped after 15 min. The hydrolytic product AB-PINACA-COOH was quantified and the formation compared to a positive control without inhibitor. Values represent mean ± S.E.M (n = 3).

Physostigmine, a general serine esterase inhibitor, potently inhibits AADAC, BChE, AChE, and CES2, but also has weak inhibitory potential on CES1.[46–48] Thus, the fact that physostigmine only has minor inhibitory potential on AB-PINACA hydrolysis, corroborates the finding that plasma esterases cannot hydrolyze this compound. The minor impact of physostigmine on PB-22 hydrolysis is likely a result of weak CES1 inhibition and/or CES2 inhibition.

Taken together, the results demonstrate that carboxylesterases are the main liver- and lung-residing esterases responsible for metabolizing AB-PINACA. Furthermore, due to loperamide and physostigmine showing only minor inhibition even at 100 μM, CES1 is likely to be the major enzyme hydrolyzing AB-PINACA in human liver and lung.

Inhibition of PB-22 hydrolysis in HLM and HPM

PB-22 was tested in the same setup as AB-PINACA described in the previous section. The results are shown in Figure 11. The inhibition pattern was comparable to that of AB-PINACA, with benzil being the only potent inhibitor. A minor, concentration-dependent inhibition was seen for physostigmine. Thus, the conclusion can be reached, that CES1 is the major hydrolytic enzyme involved in the metabolism of PB-22 in human liver and lung. Additionally, due to the close structural similarity of PB-22 to 5F-PB-22 and BB-22, this conclusion can likely be extrapolated to these compounds.

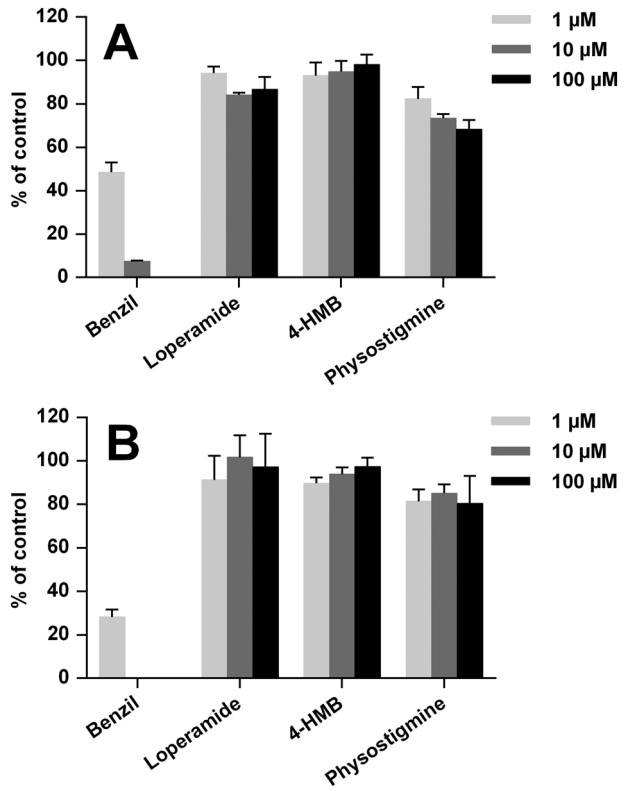

Figure 11. Effect of different selective chemical esterase inhibitors on the hydrolysis of PB-22 in HLM (A) and HPM (B). Five µM substrate was added after 5 min pre-incubation of 1, 10, or 100 µM inhibitor with 200 µg/mL HLM or HPM. Reactions were stopped after 20 min. The hydrolytic product PI-COOH was quantified and the formation compared to a positive control without inhibitor. Values represent mean ± S.E.M (n = 3).

Conclusion and perspectives

In the present paper we described the phase I metabolism of the two synthetic cannabinoids AB-PINACA and AB-FUBINACA. A major metabolic pathway of both AB-PINACA and AB-FUBINACA was CES1-mediated hydrolysis of the primary amide to AB-PINACA-COOH (M1) and AB-FUBINACA-COOH (M1), respectively. For AB-PINACA, the primary oxidative pathway was mono-hydroxylation of the N-pentyl chain to M5, while for AB-FUBINACA, which lacks an N-pentyl chain, the only major oxidative metabolite was M4 with a hydroxyl group at the 1-amino-3-methyl-1-oxobutane moiety.

It should be noted, that for metabolites other than M1, the chemical structures have not been unequivocally verified. Structure elucidation by interpretation of MS spectra provides strong clues as to the chemical structure of a molecule; however, the structure should be verified by analysis of synthesized reference compounds or nuclear magnetic resonance (NMR) analysis.

The present study provides evidence at the in vitro level using incubations with HLM. Such studies provide an indication of which phase I metabolites can be expected to be formed in vivo. The metabolites identified are likely to be subject to subsequent phase II metabolism. One of the most prevalent phase II reactions is conjugation with glucuronic acid.[49] Nucleophilic groups, such as a hydroxy or carboxy group, are conjugated, and the glucuronidated metabolites subsequently excreted into urine. However, it is recommended practice in forensic laboratories to treat urine samples with glucuronidase, sometimes combined with sulfatase, prior to analysis,[50] which leads to phase I metabolites being liberated and still being relevant targets for analytical methods. The identified metabolites are therefore likely to be useful in forensic and clinical screening of biological samples, which will provide confirmation of the metabolic pathways described in this paper.

For the two quinolineindole synthetic cannabinoids, PB-22 and 5F-PB-22, the primary metabolic pathway was previously found to consist of hydrolysis of the ester linkage, resulting in metabolites PI-COOH and 5F-PI-COOH, respectively. We demonstrate CES1 to be the major enzyme responsible for this transformation in human liver and lung, and also show CES1 to be capable of a similar transformation of the closely related compound BB-22. Thus, we revealed a key role of hepatic and pulmonary CES1 in the metabolism of the two groups of synthetic cannabinoids.

The phase I metabolism of previous JWH-type synthetic cannabinoids has been shown to be dominated by oxidative metabolism. Hydroxylation of N-alkyl chains, similar to the hydroxylation of the N-pentyl chain in AB-PINACA, has been demonstrated to be a major metabolic pathway for compounds such as JWH-018, JWH-073, XLR-11, AKB-48 and 5F-AKB-48 (Figure 1).[51–54] Other aliphatic or aromatic moieties are also hydroxylated, for example the adamantyl moiety in 5F-AKB-48 and AKB-48,[53,54] the tetramethylcyclopropyl moiety in XLR-11,[52] and the indole moiety in JWH-018 and JWH-073.[51]

The present study highlights the fact that the increasing structural diversity of newer types of synthetic cannabinoids can lead to non-CYP-mediated biotransformations dominating. Especially compounds containing ester or amide bonds are disposed to metabolism by carboxylesterases such as CES1, and hydrolyzed metabolites should be included in forensic and toxicological screening methods targeting such compounds.

Acknowledgements

This work is part of the INDICES research collaboration (Individualized drug therapy based on pharmacogenomics: Focus on carboxylesterase 1, CES1) and financed by the Danish Council for Strategic Research, Programme Commission on Individuals, Disease and Society [Grant 10-092792/DSF].

References

[1] Y. Gaoni, R. Mechoulam. Isolation, structure, and partial synthesis of an active constituent of hashish. *J. Am. Chem. Soc.* **1964**, *86*, 1646.
[2] L.A. Matsuda, S.J. Lolait, M.J. Brownstein, A.C. Young, T.I. Bonner. Structure of a cannabinoid receptor and functional expression of the cloned cDNA. *Nature* **1990**, *346*, 561.
[3] S. Munro, K.L. Thomas, M. Abu-Shaar. Molecular characterization of a peripheral receptor for cannabinoids. *Nature* **1993**, *365*, 61.
[4] R. Sedefov, A. Gallegos, L. King, D. Lopez, V. Auwärter, B. Hughes, P. Griffiths. Understanding the 'Spice' phenomenon, EMCDDA, **2009**.
[5] N. Uchiyama, R. Kikura-Hanajiri, N. Kawahara, Y. Haishima, Y. Goda. Identification of a cannabinoid analog as a new type of designer drug in a herbal product. *Chem. Pharm. Bull. (Tokyo)* **2009**, *57*, 439.
[6] V. Auwärter, S. Dresen, W. Weinmann, M. Müller, M. Pütz, N. Ferreirós. "Spice" and other herbal blends: Harmless incense or cannabinoid designer drugs? *J. Mass Spectrom.* **2009**, *44*, 832.
[7] L. Fattore, W. Fratta. Beyond THC: The new generation of cannabinoid designer drugs. *Front. Behav. Neurosci.* **2011**, *5*, 60.
[8] Danish Ministry of Health. Nr. 778 Bekendtgørelse om ændring af bekendtgørelse om euforiserende stoffer. Available at: https://www.retsinformation.dk/Forms/R0710.aspx?id=142729 [29 July 2014].
[9] Drug Enforcement Administration. Schedules of controlled substances: Temporary placement of four synthetic cannabinoids into Schedule I. Final order. *Fed. Regist.* **2014**, *79*, 7577.
[10] N. Uchiyama, S. Matsuda, M. Kawamura, R. Kikura-Hanajiri, Y. Goda. Two new-type cannabimimetic quinolinyl carboxylates, QUPIC and QUCHIC,

two new cannabimimetic carboxamide derivatives, ADB-FUBINACA and ADBICA, and five synthetic cannabinoids detected with a thiophene derivative α-PVT and an opioid receptor agonist AH-79. *Forensic Toxicol.* **2013**, *31*, 223.

[11] G. Behonick, K.G. Shanks, D.J. Firchau, G. Mathur, C.F. Lynch, M. Nashelsky, D.J. Jaskierny, C. Meroueh. Four postmortem case reports with quantitative detection of the synthetic cannabinoid, 5F-PB-22. *J. Anal. Toxicol.* **2014**, *38*, 559.

[12] N. Uchiyama, S. Matsuda, D. Wakana, R. Kikura-Hanajiri, Y. Goda. New cannabimimetic indazole derivatives, N-(1-amino-3-methyl-1-oxobutan-2-yl)-1-pentyl-1H-indazole-3-carboxamide (AB-PINACA) and N-(1-amino-3-methyl-1-oxobutan-2-yl)-1-(4-fluorobenzyl)-1H-indazole-3-carboxamide (AB-FUBINACA) identified as designer drugs i. *Forensic Toxicol.* **2013**, *31*, 93.

[13] A.A. Monte, A.C. Bronstein, D.J. Cao, K.J. Heard, J.A. Hoppe, C.O. Hoyte, J. L. Iwanicki, E.J. Lavonas. An outbreak of exposure to a novel synthetic cannabinoid. *New Engl. J. Med.* **2014**, *370*, 389.

[14] I. Buchler, M. Hayes, S. Hegde, S. Hockerman, S. Jones, S. Kortum, J. Rico, R. Tenbrink, K. Wu. Indazole derivatives as CB1 receptor modulators their preparation and use in the treatment of CB1-mediated diseases. Patent No. WO/2009/106982, **2009**.

[15] M.M. Aung, G. Griffin, J.W. Huffman, M. Wu, C. Keel, B. Yang, V. M. Showalter, M.E. Abood, B.R. Martin. Influence of the N-1 alkyl chain length of cannabimimetic indoles upon CB(1) and CB(2) receptor binding. *Drug Alcohol Depend.* **2000**, *60*, 133.

[16] A. Wohlfarth, A.S. Gandhi, S. Pang, M. Zhu, K.B. Scheidweiler, M. A. Huestis. Metabolism of synthetic cannabinoids PB-22 and its 5-fluoro analog, 5F-PB-22, by human hepatocyte incubation and high-resolution mass spectrometry. *Anal. Bioanal. Chem.* **2014**, *406*, 1763.

[17] T. Takayama, M. Suzuki, K. Todoroki, K. Inoue, J.Z. Min, R. Kikura-Hanajiri, Y. Goda, T. Toyo'oka. UPLC/ESI-MS/MS-based determination of metabolism of several new illicit drugs, ADB-FUBINACA, AB-FUBINACA, AB-PINACA, QUPIC, 5F-QUPIC and α-PVT, by human liver microsome. *Biomed. Chromatogr.* **2014**, *28*, 831.

[18] T. Fukami, T. Yokoi. The emerging role of human esterases. *Drug Metab. Pharmacokinet.* **2012**, *27*, 466.

[19] J. Massoulié, L. Pezzementi, S. Bon, E. Krejci, F.M. Vallette. Molecular and cellular biology of cholinesterases. *Prog. Neurobiol.* **1993**, *41*, 31.

[20] A. Tunek, E. Levin, L.A. Svensson. Hydrolysis of 3H-bambuterol, a carbamate prodrug of terbutaline, in blood from humans and laboratory animals *in vitro*. *Biochem. Pharmacol.* **1988**, *37*, 3867.

[21] C. Mattes, R. Bradley, E. Slaughter, S. Browne. Cocaine and butyrylcholinesterase (BChE): Determination of enzymatic parameters. *Life Sci.* **1996**, *58*, PL257.

[22] T. Satoh, P. Taylor, W.F. Bosron, S.P. Sanghani, M. Hosokawa, B.N. La Du. Current progress on esterases: From molecular structure to function. *Drug Metab. Dispos.* **2002**, *30*, 488.

[23] R. Thomsen, H.B. Rasmussen, K. Linnet. In vitro drug metabolism by human carboxylesterase 1: Focus on angiotensin-converting enzyme inhibitors. *Drug Metab. Dispos.* **2014**, *42*, 126.

[24] Z. Sun, D.J. Murry, S.P. Sanghani, W.I. Davis, N.Y. Kedishvili, Q. Zou, T. D. Hurley, W.F. Bosron. Methylphenidate is stereoselectively hydrolyzed by human carboxylesterase CES1A1. *J. Pharmacol. Exp. Ther.* **2004**, *310*, 469.

[25] D. Shi, J. Yang, D. Yang, E.L. LeCluyse, C. Black, L. You, F. Akhlaghi, B. Yan. Anti-influenza prodrug oseltamivir is activated by carboxylesterase human carboxylesterase 1, and the activation is inhibited by antiplatelet agent clopidogrel. *J. Pharmacol. Exp. Ther.* **2006**, *319*, 1477.

[26] E.T. Williams, J.E. Carlson, W.G. Lai, Y.N. Wong, T. Yoshimura, D.J. Critchley, M. Narurkar. Investigation of the metabolism of rufinamide and its interaction with valproate. *Drug Metab. Lett.* **2011**, *5*, 280.

[27] M. Tang, M. Mukundan, J. Yang, N. Charpentier, E.L. LeCluyse, C. Black, D. Yang, D. Shi, B. Yan. Antiplatelet agents aspirin and clopidogrel are hydrolyzed by distinct carboxylesterases, and clopidogrel is transesterificated in the presence of ethyl alcohol. *J. Pharmacol. Exp. Ther.* **2006**, *319*, 1467.

[28] J. Zhang, J.C. Burnell, N. Dumaual, W.F. Bosron. Binding and hydrolysis of meperidine by human liver carboxylesterase hCE-1. *J. Pharmacol. Exp. Ther.* **1999**, *290*, 314.

[29] S.C. Laizure, R.B. Parker, V.L. Herring, Z.-Y. Hu. Identification of carboxylesterase-dependent dabigatran etexilate hydrolysis. *Drug Metab. Dispos.* **2014**, *42*, 201.

[30] R. Humerickhouse, K. Lohrbach, L. Li, W.F. Bosron, M.E. Dolan. Characterization of CPT-11 hydrolysis by human liver carboxylesterase isoforms hCE-1 and hCE-2. *Cancer Res.* **2000**, *60*, 1189.

[31] E.T. Williams, K.O. Jones, G.D. Ponsler, S.M. Lowery, E.J. Perkins, S. A. Wrighton, K.J. Ruterbories, M. Kazui, N.A. Farid. The biotransformation of prasugrel, a new thienopyridine prodrug, by the human carboxylesterases 1 and 2. *Drug Metab. Dispos.* **2008**, *36*, 1227.

[32] Y. Kobayashi, T. Fukami, M. Shimizu, M. Nakajima, T. Yokoi. Contributions of arylacetamide deacetylase and carboxylesterase 2 to flutamide hydrolysis in human liver. *Drug Metab. Dispos.* **2012**, *40*, 1080.

[33] A. Nakajima, T. Fukami, Y. Kobayashi, A. Watanabe, M. Nakajima, T. Yokoi. Human arylacetamide deacetylase is responsible for deacetylation of rifamycins: Rifampicin, rifabutin, and rifapentine. *Biochem. Pharmacol.* **2011**, *82*, 1747.

[34] A. Watanabe, T. Fukami, S. Takahashi, Y. Kobayashi, N. Nakagawa, M. Nakajima, T. Yokoi. Arylacetamide deacetylase is a determinant enzyme for the difference in hydrolase activities of phenacetin and acetaminophen. *Drug Metab. Dispos.* **2010**, *38*, 1532.

[35] D.I. Draganov, J.F. Teiber, A. Speelman, Y. Osawa, R. Sunahara, B. N. La Du. Human paraoxonases (PON1, PON2, and PON3) are lactonases with overlapping and distinct substrate specificities. *J. Lipid Res.* **2005**, *46*, 1239.

[36] E.K. Tarkiainen, J.T. Backman, M. Neuvonen, P.J. Neuvonen, M. Schwab, M. Niemi. Carboxylesterase 1 polymorphism impairs oseltamivir bioactivation in humans. *Clin. Pharmacol. Ther.* **2012**, *92*, 68.

[37] M.C. McGuire, C.P. Nogueira, C.F. Bartels, H. Lightstone, A. Hajra, A. F. Van der Spek, O. Lockridge, B.N. La Du. Identification of the structural mutation responsible for the dibucaine-resistant (atypical) variant form of human serum cholinesterase. *Proc. Natl. Acad. Sci. U. S. A.* **1989**, *86*, 953.

[38] L.G. Costa, G. Giordano, T.B. Cole, J. Marsillach, C.E. Furlong. Paraoxonase 1 (PON1) as a genetic determinant of susceptibility to organophosphate toxicity. *Toxicology* **2013**, 307, 115.

[39] G.L. Ellman, K.D. Courtney, V. Andres, R.M. Feather-Stone. A new and rapid colorimetric determination of acetylcholinesterase activity. *Biochem. Pharmacol.* **1961**, *7*, 88.

[40] L. Austin, W.K. Berry. Two selective inhibitors of cholinesterase. *Biochem. J.* **1953**, *54*, 695.

[41] P. Eyer, F. Worek, D. Kiderlen, G. Sinko, A. Stuglin, V. Simeon-Rudolf, E. Reiner. Molar absorption coefficients for the reduced Ellman reagent: Reassessment. *Anal. Biochem.* **2003**, *312*, 224.

[42] E.T. Williams, M.E. Ehsani, X. Wang, H. Wang, Y.-W. Qian, S.A. Wrighton, E.J. Perkins. Effect of buffer components and carrier solvents on in vitro activity of recombinant human carboxylesterases. *J. Pharmacol. Toxicol. Methods* **2008**, *57*, 138.

[43] R.M. Wadkins, J.L. Hyatt, X. Wei, K.J.P. Yoon, M. Wierdl, C.C. Edwards, C. L. Morton, J.C. Obenauer, K. Damodaran, P. Beroza, M.K. Danks, P. M. Potter. Identification and characterization of novel benzil (diphenylethane-1,2-dione) analogues as inhibitors of mammalian carboxylesterases. *J. Med. Chem.* **2005**, *48*, 2906.

[44] S.K. Quinney, S.P. Sanghani, W.I. Davis, T.D. Hurley, Z. Sun, D.J. Murry, W. F. Bosron. Hydrolysis of capecitabine to 5 -Deoxy-5-fluorocytidine by human carboxylesterases and inhibition by loperamide. *Pharmacology* **2005**, *313*, 1011.

[45] R.C. Sorenson, S.L. Primo-Parmo, C.L. Kuo, S. Adkins, O. Lockridge, B. N. La Du. Reconsideration of the catalytic center and mechanism of mammalian paraoxonase/arylesterase. *Proc. Natl. Acad. Sci. U. S. A.* **1995**, *92*, 7187.

[46] A. Watanabe, T. Fukami, M. Nakajima, M. Takamiya, Y. Aoki, T. Yokoi. Human arylacetamide deacetylase is a principal enzyme in flutamide hydrolysis. *Drug Metab. Dispos.* **2009**, *37*, 1513.

[47] E.V. Pindel, N.Y. Kedishvili, T.L. Abraham, M.R. Brzezinski, J. Zhang, R. A. Dean, W.F. Bosron. Purification and cloning of a broad substrate specificity human liver carboxylesterase that catalyzes the hydrolysis of cocaine and heroin. *J. Biol. Chem.* **1997**, *272*, 14769.

[48] D.J. Triggle, J.M. Mitchell, R. Filler. The pharmacology of physostigmine. *CNS Drug Rev.* **1998**, *4*, 87.

[49] P.G. Wells, P.I. Mackenzie, J.R. Chowdhury, C. Guillemette, P.A. Gregory, Y. Ishii, A.J. Hansen, F.K. Kessler, P.M. Kim, N.R. Chowdhury, J.K. Ritter. Glucuronidation and the UDP-glucuronosyltransferases in health and disease. *Drug Metab. Dispos.* **2004**, *32*, 281.

[50] A. Negrusz, G. Cooper. *Clarke's Analytical Forensic Toxicology*. Pharmaceutical Press: London, **2013**.

[51] M.A. ElSohly, W. Gul, K.M. Elsohly, T.P. Murphy, V.L.M. Madgula, S.I. Khan. Liquid chromatography-tandem mass spectrometry analysis of urine specimens for K2 (JWH-018) metabolites. *J. Anal. Toxicol.* **2011**, *35*, 487.

[52] A. Wohlfarth, S. Pang, M. Zhu, A.S. Gandhi, K.B. Scheidweiler, H. Liu, M. A. Huestis. First metabolic profile of XLR-11, a novel synthetic

cannabinoid, obtained by using human hepatocytes and high-resolution mass spectrometry. *Clin. Chem.* **2013**, *59*, 1638.

[53] A.S. Gandhi, M. Zhu, S. Pang, A. Wohlfarth, K.B. Scheidweiler, H. Liu, M. A. Huestis. First characterization of AKB-48 metabolism, a novel synthetic cannabinoid, using human hepatocytes and high-resolution mass spectrometry. *AAPS J.* **2013**, *15*, 1091.

[54] N.B. Holm, A.J. Pedersen, P.W. Dalsgaard, K. Linnet. Metabolites of 5F-AKB-48, a synthetic cannabinoid receptor agonist, identified in human urine and liver microsomal preparations using liquid chromatography high-resolution mass spectrometry. *Drug Test. Anal.* **2014**. DOI: 10.1002/dta.1663

Appendix A

List of all partners in the INDICES consortium:

Henrik Berg Rasmussen, Institute of Biological Psychiatry, Mental Health Centre Sct. Hans, Copenhagen University Hospital, Roskilde, Denmark.

Ditte Bjerre, Institute of Biological Psychiatry, Mental Health Centre Sct. Hans, Copenhagen University Hospital, Roskilde, Denmark.

Majbritt Busk Madsen, Institute of Biological Psychiatry, Mental Health Centre Sct. Hans, Copenhagen University Hospital, Roskilde, Denmark.

Laura Ferrero, Institute of Biological Psychiatry, Mental Health Centre Sct. Hans, Copenhagen University Hospital, Roskilde, Denmark.

Kristian Linnet, Section of Forensic Chemistry, Department of Forensic Medicine, Faculty of Health and Medical Sciences, University of Copenhagen, Denmark.

Ragnar Thomsen, Section of Forensic Chemistry, Department of Forensic Medicine, Faculty of Health and Medical Sciences, University of Copenhagen, Denmark.

Gesche Jürgens, Department of Clinical Pharmacology, Bispebjerg University Hospital, Copenhagen, Denmark.

Kim Dalhoff, Department of Clinical Pharmacology, Bispebjerg University Hospital, Copenhagen, Denmark.

Claus Stage, Department of Clinical Pharmacology, Bispebjerg University Hospital, Copenhagen, Denmark.

Hreinn Stefansson, CNS Division, deCODE Genetics, Reykjavik, Iceland.

Thomas Hankemeier, The Leiden/Amsterdam Center for Drug Research LACDR, Leiden University, Gorlaeus laboratories, Leiden, The Netherlands.

Rima Kaddurah-Daouk, Department of Psychiatry and Behavioral Sciences, Duke University, Durham, NC, USA.

Søren Brunak, Center for Biological Sequence Analysis, Technical University of Denmark, Kgs. Lyngby, Denmark.

Olivier Taboureau, Center for Biological Sequence Analysis, Technical University of Denmark, Kgs. Lyngby, Denmark.

Grace Shema Nzabonimpa, Center for Biological Sequence Analysis, Technical University of Denmark, Kgs. Lyngby, Denmark.

Tine Houmann, Centre for Child and Adolescent Mental Health, Mental Health Services in the Capital Region of Denmark.

Pia Jeppesen, Centre for Child and Adolescent Mental Health, Mental Health Services in the Capital Region of Denmark.

Kristine Kaalund-Jørgesen, Centre for Child and Adolescent Mental Health, Mental Health Services in the Capital Region of Denmark.

Peter Riis Hansen, Department of Cardiology, Copenhagen University Hospital, Hellerup, Denmark.

Karl Emil Kristensen, Department of Cardiology, Copenhagen University Hospital, Hellerup, Denmark.

Anne Katrine Pagsberg, Centre for Child and Adolescent Mental Health, Mental Health Services in the Capital Region of Denmark.

Kerstin Plessen, Centre for Child and Adolescent Mental Health, Mental Health Services in the Capital Region of Denmark.

Poul-Erik Hansen, Department of Science, Systems and Models, Roskilde University, Roskilde, Denmark.

Thomas Werge, Institute of Biological Psychiatry, Mental Health Centre Sct. Hans, Copenhagen University Hospital, Roskilde, Denmark.

Jørgen Dyrborg, Centre for Child and Adolescent Mental Health, Mental Health Services in the Capital Region of Denmark.

Maj-Britt Lauritzen, Centre for Child and Adolescent Mental Health, Mental Health Services in the Capital Region of Denmark.

Supporting information

Additional supporting information may be found in the online version at the publisher's web site.